J. Phys. Chem. A **2009,** *113,* 7133–7137

Acceptor Tunneling Motion and O−H Stretching Vibration Overtones of the Water Dimer

Vesa Hänninen, Teemu Salmi, and Lauri Halonen*

Laboratory of Physical Chemistry, University of Helsinki, P.O. Box 55 (A.I. Virtasen aukio 1),
FIN-00014 Helsinki, Finland

Received: March 4, 2009; Revised Manuscript Received: April 27, 2009

We have carried out a detailed investigation of the acceptor tunneling in the water dimer. This motion is responsible for the largest splitting of vibrational states in the dimer, the so-called acceptor splitting. Our results confirm that this splitting is due to a coupled 2-fold motion: The internal rotation of the donor with respect to the O−O axis, and the wagging of the acceptor. The minimum potential energy path along the corresponding coordinate was computed using the coupled-cluster ab initio with single, double, and perturbative triple excitations (CCSD(T)) method and the augmented correlation consistent polarized valence quadruple ζ basis set (aug-cc-pVQZ). The pure acceptor tunneling energy levels were obtained by the variational method with a free rotor basis. The acceptor splittings associated with the O−H stretching overtone states of the water dimer were calculated with a simple model which employs adiabatic separation between the tunneling motion and high-frequency vibrations.

Introduction

The importance of water clusters cannot be underestimated. Understanding the bonding in water clusters is valuable for the theory of intermolecular forces.[1] Water clusters also play a role in many atmospheric phenomena. Especially, the role of water in the atmospheric heat balance, i.e., the greenhouse effect, has been a subject of a large amount of scientific research. These studies have mainly concentrated on the simplest water cluster, the water dimer. It has been speculated that the water dimer is an important light absorber in the atmosphere and could contribute to the excess solar absorption and so-called "water continuum" absorption.[2,3] In the latter, the absorption bands of water in the far-infrared region possess broad structures, the origin of which is under debate. One possible contribution to these bands arises from the low-frequency internal motions of water clusters.

The spectroscopy of the water dimer has been studied extensively in the past. Water dimer vibration−rotation spectra at nonequilibrium laboratory conditions have yielded a large amount of accurate information on the geometry and energy level structure.[4−17] Most of these studies have concentrated on the low-frequency vibrations but some published work also exists on the O−H stretching fundamentals and the first O−H stretching overtones.[12,13,15,16,18,19] Some earlier attempts to observe the water dimer in the atmosphere have failed,[20,21] but later there has been a reported observation in the high O−H stretching overtone region[22] although this result has been challenged.[23,24] However, two recent laboratory measurements of the water continuum absorption near atmospheric sample conditions indicate the presence of the water dimer.[19,25]

Computational water dimer studies have concentrated on two areas: intramolecular motions (bond stretchings and valence angle bendings) and large amplitude intermolecular motions. Full variational treatment of vibrations in the water dimer including highly exited O−H stretching states is impossible at the moment due to the large density of states. Therefore, approximations should be employed if the inter- and intramolecular motions are treated simultaneously. One commonly used approach is the adiabatic approximation that separates the slow large amplitude motions from the fast high-frequency vibrations. This method has been successfully employed for the water dimer[26] and in some studies of molecules exhibiting large amplitude motions.[27,28] It is commonly observed that the tunneling splittings associated with high-frequency fundamental and overtone regions show variation in the size of the splitting.[29] For the water dimer, these kinds of splittings have not yet been assigned.

Curvilinear internal coordinate approach is a good way to model overtone vibrations and large amplitude motions in polyatomic molecules.[27,30−32] The main advantages of this method compared to the rectilinear normal coordinate approach are the simpler potential energy expressions and better representation of vibrational motions in the case of weakly coupled oscillators. On the other hand, complicated forms of the kinetic energy operator are a drawback. The gradients of the coordinates with respect to the positions of nuclei must be calculated in order to form the kinetic energy operator. The conventional Wilson's s-vector method[33] is not practical if the expressions for the coordinates are complicated, which is often the case for the coordinates of large amplitude motions. Fortunately, a novel method, which employs the branch of mathematics called geometric algebra, has been developed to obtain the gradients.[34,35]

The water dimer exhibits three large amplitude vibrations that tunnel through potential energy barriers. These motions are referred to in literature as acceptor tunneling, donor−acceptor interchange, and bifurcation tunneling.[36] The barrier for the acceptor tunneling is the lowest giving rise to the largest splitting, 11.18 cm^{-1} in the ground vibrational state of $(H_2O)_2$.[37] The two other splittings are significantly smaller in magnitude. Recently, a full-dimensional potential energy surface for the water dimer has been constructed using the coupled-cluster ab initio method with single, double, and perturbative triple excitations (CCSD(T)) and correlation consistent polarized valence triple ζ basis set (aug-cc-pVTZ).[17] With this surface, the intermonomer vibration−rotation tunneling (VRT) levels were calculated employing the coupled-channel scattering

---

* Corresponding author, lauri.halonen@helsinki.fi.

10.1021/jp901974z CCC: $40.75

method. This involves a fully coupled treatment of all six intermolecular degrees of freedom, but the intramolecular structure has been kept frozen at the equilibrium values (the rigid monomer approximation). Their calculated value for the acceptor tunneling splitting was 13.47 cm^{-1} for $(H_2O)_2$ and 2.41 cm^{-1} for $(D_2O)_2$.

The O−H stretching and H−O−H bending overtone spectra of the water dimer have been studied computationally.[38−40] The spectra have been simulated by employing models where the monomers have been treated as separate oscillators; i.e., the couplings between the monomers have been neglegted. This separation is justified because the vibrations in the two water monomer units (denoted as an asymmetric donor and a symmetric acceptor) are weakly coupled to the large amplitude vibrations of the dimer. The interactions between high-frequency vibrations of different monomers are also weak.[38] Therefore, a simpler model can be used where the large amplitude vibrations are frozen such that the corresponding coordinates are constrained to the equilibrium values and the coupling terms between the O−H stretching and the H−O−H bending vibrations of the different monomer units are excluded in the vibrational Hamiltonian.[39] In our recent work,[40] the potential energy surfaces have been computed with high-level ab initio methods. We have employed within the Born−Oppenheimer approximation exact kinetic energy operators for the monomer units and calculated potential energy surfaces using the CCSD(T) electronic structure calculation method with augmented correlation consistent polarized valence triple and quadruple ζ basis sets (aug-cc-pVTZ and aug-cc-pVQZ) of Dunning and co-workers.[41,42] In addition, the extrapolation method to the complete basis set (CBS) limit, core valence electron correlation corrections, and second-order relativistic corrections were included to improve the energy. Still, there remain discrepancies between theoretical and experimental vibrational term values in the case of the hydrogen bonded O−H stretching fundamental vibrational energy. The difference between the observed versus calculated value is around 40 cm^{-1}. It is well-known that the coupled cluster theory yields vibrational fundamentals with a precision of a few wavenumbers. Therefore, the origin of this discrepancy lies elsewhere. The vibrational model includes no coupling between the high-frequency vibrations between the monomers. These couplings are small and cannot account for the large discrepancy. However, the couplings between the intramolecular and intermolecular motions can be larger. Thus, the incompleteness of the vibrational model may cause inaccurate energies. It is challenging to find the solution to the problem if the deviation is due to a combination of several effects. It is also possible that there exists some specific strong coupling that is missing from the model. Schofield et al.[43] studied the interaction between the hydrogen bonded O−H stretching vibration and O−O bond distance. They found out that this interaction cannot solely account for the discrepancy.

The aim of this work is to study the interaction between the intermolecular large amplitude acceptor tunneling motion and the intramolecular high-frequency vibrations. We simulate the acceptor tunneling and overtone O−H stretching states of the water dimer using a model that excludes the other low-energy vibrations. As the acceptor tunneling coordinate, we have chosen an intermolecular dihedral angle which represents simultaneously both the torsion of the donor and the wagging of the acceptor. The splitting caused by this tunneling motion is well documented experimentally.[37] Geometric algebra approach is employed in the derivation of the kinetic energy operator for the acceptor tunneling motion. The tunneling energies are calculated variationally using a free rotor basis. The adiabatic approximation is employed in the calculation of the interaction between the large amplitude motion and the high-frequency vibrations.

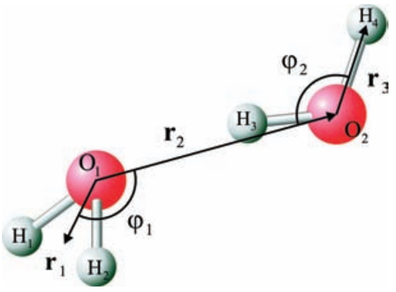

Figure 1. Water dimer coordinates.

Theoretical Model

The vibration−rotation Hamiltonian of an N-atomic molecule can be written in the Cartesian representation as

$$H = T + V = -\frac{\hbar^2}{2}\sum_{\alpha=1}^{N}\frac{\nabla_\alpha^{\;2}}{m_\alpha} + V \qquad (1)$$

where the summation index α is over the nuclei, ∇_α is the gradient operator with respect to the position of the nucleus α, N is the number of the nuclei, m_α is the mass of the αth nucleus, and V is the potential energy function. When the translational motion and the angular momentum components of the Hamiltonian are omitted, the kinetic energy T of the vibrational motion can be expressed as

$$T = -\frac{\hbar^2}{2}\sum_{i,j=1}^{3N-6}\left(\frac{\partial}{\partial q_i}+\frac{1}{J}\frac{\partial J}{\partial q_i}\right)g^{(q_iq_j)}\frac{\partial}{\partial q_j} \qquad (2)$$

where the summations are over the generalized coordinates and the quantities

$$g^{(q_iq_j)} = \sum_{\alpha=1}^{N}\frac{1}{m_\alpha}(\nabla_\alpha q_i)\cdot(\nabla_\alpha q_j) \qquad (3)$$

are the elements of the mass-weighted reciprocal metric tensor, whose values are Wilson's g-matrix elements when evaluated at the reference position. The volume element of integration is $d\tau = J\, dq_1\, dq_2$ ..., where the weight function J is the Jacobian of the coordinate transformation. The kinetic energy of our work is transformed into a form with a unit weight function.[35]

It is not practical to use an exact kinetic energy operator for all degrees of motion in the water dimer. The inclusion of the relative motions of monomers is demanding in constructing an appropriate Hamiltonian operator. In order to find an approximate solution to the vibrational eigenvalue problem, we adopt a vibrationally adiabatic approach where the low-frequency tunneling motion is separated from the high-frequency vibrations. Thus, the large amplitude acceptor tunneling motion problem is solved one-dimensionally. The definition of the tunneling coordinate is such that it can be described as a 2-fold motion of the wagging of the acceptor $H_1O_1H_2$ and an internal rotation of the donor $H_3O_2H_4$ (see Figure 1). Instead of the standard vector algebra, a more general approach, geometric algebra, is used in the following derivations. An introduction

TABLE 1: Acceptor Tunneling Potential Energy Parameters of the Water Dimer (in cm^{-1})

V_0	V_2	V_4	V_6
77.6914	−77.7518	3.78392	−3.4087

to geometric algebra and various molecular applications can be found in a review article.[35]

The cosine of the acceptor tunneling coordinate is defined as the cosine of an angle between the planes $\mathbf{i}_1$ and $\mathbf{i}_2$ (see Figure 1)

$$\cos \xi = \mathbf{i}_1 \cdot \mathbf{i}_2 \tag{4}$$

where the planes are mathematically expressed as

$$\mathbf{i}_1 = \frac{\mathbf{u}_{\mathbf{r}_1} \wedge \mathbf{u}_{\mathbf{r}_2}}{\sin \varphi_1} \tag{5}$$

$$\mathbf{i}_2 = \frac{\mathbf{u}_{\mathbf{r}_2} \wedge \mathbf{u}_{\mathbf{r}_3}}{\sin \varphi_2} \tag{6}$$

The quantity φ_1 is the wagging angle and φ_2 is the $O_1-O_2-H_4$ angle. The vector $\mathbf{u}_{\mathbf{r}_1}$, written in terms of unit bond vectors, is

$$\mathbf{u}_{\mathbf{r}_1} = \frac{1}{2}(\mathbf{u}_{\mathbf{r}_{\mathbf{O}_1\mathbf{H}_1}} + \mathbf{u}_{\mathbf{r}_{\mathbf{O}_1\mathbf{H}_2}}) \tag{7}$$

The quantities $\mathbf{u}_{\mathbf{r}_2}$ and $\mathbf{u}_{\mathbf{r}_3}$ are equal to the unit vectors $\mathbf{u}_{\mathbf{r}_{\mathrm{O1O2}}}$ and $\mathbf{u}_{\mathbf{r}_{\mathrm{O2H4}}}$, respectively. The vector $\mathbf{r}_1$ specifies the position of an imaginary atom X with the mass of $2m_{\mathrm{H}}$. The eq 4 can be written as

$$\begin{aligned}
\cos \xi &= \frac{\mathbf{u}_{\mathbf{r}_1} \wedge \mathbf{u}_{\mathbf{r}_2}}{\sin \varphi_1} \cdot \frac{\mathbf{u}_{\mathbf{r}_2} \wedge \mathbf{u}_{\mathbf{r}_3}}{\sin \varphi_2} \\
&= \frac{\mathbf{u}_{\mathbf{r}_2} \cdot \mathbf{u}_{\mathbf{r}_2} \mathbf{u}_{\mathbf{r}_1} \cdot \mathbf{u}_{\mathbf{r}_3} - \mathbf{u}_{\mathbf{r}_1} \cdot \mathbf{u}_{\mathbf{r}_2} \mathbf{u}_{\mathbf{r}_2} \cdot \mathbf{u}_{\mathbf{r}_3}}{\sin \varphi_1 \sin \varphi_2} \\
&= \frac{\mathbf{u}_{\mathbf{r}_1} \cdot \mathbf{u}_{\mathbf{r}_3} - \mathbf{u}_{\mathbf{r}_1} \cdot \mathbf{u}_{\mathbf{r}_2} \mathbf{u}_{\mathbf{r}_2} \cdot \mathbf{u}_{\mathbf{r}_3}}{\sin \varphi_1 \sin \varphi_2} \\
&= \frac{\mathbf{u}_{\mathbf{r}_1} \cdot \mathbf{u}_{\mathbf{r}_3} - \cos \varphi_1 \cos \varphi_2}{\sin \varphi_1 \sin \varphi_2}
\end{aligned} \tag{8}$$

where the Laplace expansion rule for the inner product of two p-blades is employed as

$$(\mathbf{a}_p \wedge \dots \wedge \mathbf{a}_1) \cdot (\mathbf{b}_p \wedge \dots \wedge \mathbf{b}_1) = \sum_{k=1}^{p} (-1)^{k+1} \times (\mathbf{a}_1 \cdot \mathbf{b}_k)(\mathbf{a}_p \wedge \dots \wedge \mathbf{a}_2) \cdot (\mathbf{b}_1 \wedge \dots \wedge \mathbf{b}_k^* \wedge \dots \wedge \mathbf{b}_p)$$

The asterisk in $\mathbf{b}_k^*$ means that the vector $\mathbf{b}_k$ is omitted from the product. Equation 8 can be rewritten as

$$\mathbf{r}_1 \cdot \mathbf{r}_3 = r_1 r_3 (\cos \xi \sin \varphi_1 \sin \varphi_2 + \cos \varphi_1 \cos \varphi_2) \tag{9}$$

The derivatives $\partial_{\mathbf{x}_{\mathrm{X}}}\xi$, $\partial_{\mathbf{x}_{\mathrm{H4}}}\xi$, $\partial_{\mathbf{x}_{\mathrm{O1}}}\xi$, and $\partial_{\mathbf{x}_{\mathrm{O2}}}\xi$ in eq 3 can be obtained by differentiating both sides of eq 9 with respect to the atomic positions. (See Supporting Information for the derivation of the gradients.)

The interaction between the acceptor tunneling motion and the O−H stretching vibrations is treated by expressing the leading structural and potential energy parameters of the O−H stretching Hamiltonian as functions of the acceptor tunneling coordinate. The Hamiltonian is written as

$$H_{\mathbf{OH}} = H_\xi + \omega_q(\xi)\left(\nu_q + \frac{1}{2}\right) - \omega x_q(\xi)\left(\nu_q + \frac{1}{2}\right)^2 \tag{10}$$

where H_ξ is the Hamiltonian for the pure tunneling motion and the harmonic wavenumber of the high-frequency vibration is expanded as

$$\omega_q(\xi) = \omega_q^{(0)} + \omega_q^{(2)} \cos 2\xi + \omega_q^{(4)} \cos 4\xi + \dots \tag{11}$$

The index q represents the coordinate of the high-frequency vibration and ν_q is the corresponding vibrational quantum number. The acceptor tunneling dependence of the anharmonicity parameter ωx_q could be expressed similarly, but this dependence is ignored because its effect is small on the final results.

Results and Discussion

The optimized geometries of the water dimer were calculated along the large amplitude acceptor tunneling coordinate using the coupled cluster (CCSD(T)) ab initio method. The optimizations were carried out with the correlation consistent aug-cc-pVQZ basis set. The frozen core approximation was used for the 1s electrons of oxygen atoms. All the electronic structure calculations were carried out with the program MOLPRO.[44] In these computations, the structure of the water dimer is allowed to relax except for the acceptor tunneling coordinate ξ. Our calculations show that along this potential minimum energy path of the coordinate ξ the wagging angle φ_1 inverts at the transition state when the torsional angle reaches 90° thus switching the acceptor hydrogens. Therefore, the acceptor tunneling motion can be described as a 2-fold motion of the wagging and internal rotation. The one-dimensional potential energy surface of the acceptor tunneling motion can be expressed using the following simple form as

$$V(\xi) = V_0 + V_2 \cos 2\xi + V_4 \cos 4\xi + \dots \tag{12}$$

The computed energies at chosen acceptor tunneling angles are shown in Figure 2. The potential energy parameters of eq 12 obtained from computed points with the least-squares method are given in Table 1. This potential energy function was used in the tunneling Hamiltonian. The coefficient $g^{(\xi\xi)}$ in the kinetic energy operator was constrained to its equilibrium value (38.48 u^{-1} for normal and 20.53 u^{-1} for fully deuterated water dimer). This is a good approximation and it avoids the problem of singularities at some values of the angle ξ. The singularities arise from the ignored overall rotational part of the Hamiltonian. The acceptor splittings on the ground vibrational state calculated variationally using the free rotor basis which depends on ξ are given for $(H_2O)_2$ and $(D_2O)_2$ in Table 2. Basis functions with

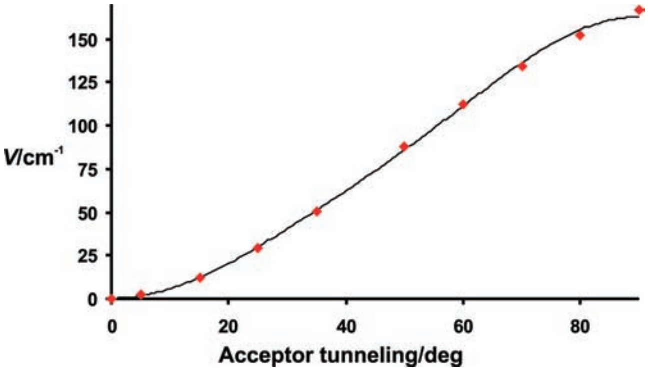

Figure 2. Acceptor tunneling potential energy surface for the water dimer.

TABLE 2: Acceptor Tunneling Splittings for the Ground Vibrational State Using the One-Dimensional Model (in cm^{-1})

dimer	calculated	experimental[a]
$(H_2O)_2$	13.04	11.18
$(D_2O)_2$	2.76	1.77

[a] From ref 37.

the quantum label $v_\xi = 0, 1, ..., 10$ produced converged eigenvalues for the lowest acceptor tunneling states.

The potential energy surfaces (PES) of the H_2O monomer unit vibrations were computed around optimized geometries at the given acceptor tunneling angles with the CCSD(T)/aug-cc-pVQZ method. The potential energy parameters were optimized with the least-squares method using computed total energy points as data. For the O−H stretching modes, the PES was obtained by calculating eight single point energies around the given geometry. The bond lengths r_i were altered by ±0.05, ±0.10, ±0.15, and ±0.20 Å. The Morse potential energy function

$$V(\Delta r) = D(1 - e^{-a\Delta r})^2 \qquad (13)$$

where D is the well depth, a is the Morse steepness parameter, $\Delta r = r - r_e$, and r_e is the equilibrium value of the bond length, was used for the O−H stretches.[45] The harmonic wavenumber ω was computed from the Morse parameters. In the case of the H−O−H bending motion, the vector bisecting the angle was kept fixed while the H−O−H angle was changed. Eight points for the bending PES were calculated changing the H−O−H angle by ±5°, ±10°, ±15°, and ±20°. The potential function was expressed as a series expansion over the angle displacement as follows

$$V(\Delta\theta) = \sum_{i=2}^{4} \frac{f_i(\Delta\theta)^i}{i!} \qquad (14)$$

where $\Delta\theta = \theta - \theta_e$ and θ_e is the equilibrium value of the H−O−H bond angle. The harmonic wavenumber ω_θ was obtained directly from the f_2 parameter. The calculated harmonic wavenumbers of stretches and bends are presented in Table 3.

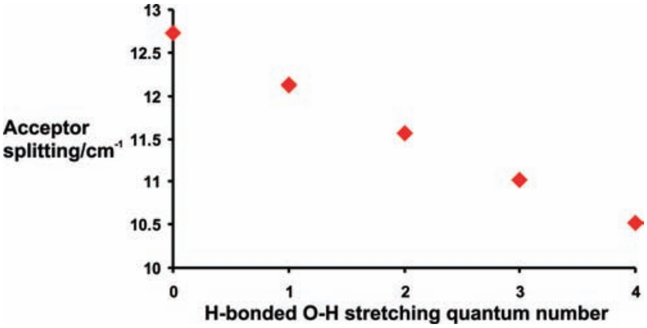

Figure 3. Acceptor splitting associated with the H-bonded O−H stretching overtone states in $(H_2O)_2$.

TABLE 4: Model Parameters (in cm^{-1}) for the Water Dimer

coordinate q	$\omega_q^{(0)}$	$\omega_q^{(2)}$	$\omega_q^{(4)}$
$r(O_2H_4)$	3928.45	−0.9278	0.2087
$r(O_2H_3)$	3797.39	−6.9238	0.4191
$r(O_1H_2)$	3914.43	−0.5277	−0.6707
$r(O_1H_1)$	3917.31	−3.7047	−0.3115
$\theta(H_1O_1H_2)$	1667.07	0.7999	0.3390
$\theta(H_3O_2H_4)$	1690.18	−3.3269	−0.9085

The tunneling splittings associated with the O−H stretching overtone states were calculated using the Hamiltonian in eq 10. The largest effect on the splitting is in the hydrogen-bonded O−H stretching vibration overtone states. The harmonic wavenumber of the bonded O−H stretch (associated with the coordinate $r(O_2H_3)$) reaches its largest value at the saddle point (see Table 3). This effectively increases the tunneling barrier when the O−H stretching vibration is excited. This phenomenon decreases the acceptor tunneling splitting associated with the O−H stretching vibration. The bonded O−H stretching quantum number dependency on the acceptor tunneling splitting can be seen in the Figure 3. Note that the splitting at the O−H stretching quantum number equal to 0 is slightly smaller than the calculated splitting when the pure acceptor tunneling Hamiltonian was used. This occurs because the zero-point energy of the O−H stretching mode varies along the acceptor tunneling coordinate. Similarly, as for the pure acceptor tunneling motion, the calculations were done with the variational method using free rotor eigenfunctions as a basis. Similar effects although smaller in magnitude can be seen in all the other O−H stretching modes and the acceptor bending mode. The model parameters for all high frequency modes are given in Table 4. The bending mode of the donor monomer shows small increasing tendency in the acceptor splitting as bending excitation increases.

Summary

In this work, we have reproduced computationally the acceptor tunneling splittings and torsional energy of the water

TABLE 3: Harmonic O−H Stretching and H−O−H Bending Wavenumbers (cm^{-1}) for the Water Dimer at Different Torsional Angles

torsional angle/deg	$\omega_{r(O_1H_1)}$	$\omega_{r(O_1H_2)}$	$\omega_{r(O_2H_4)}$	$\omega_{r(O_2H_3)}$	$\omega_{\theta(H_1O_1H_2)}$	$\omega_{\theta(H_3O_2H_4)}$
90	3921.17	3914.40	3929.56	3805.79	1666.47	1692.40
70	3919.61	3914.50	3929.29	3801.75	1666.70	1692.85
45	3916.80	3914.91	3928.01	3795.67	1666.93	1689.97
0	3913.21	3913.21	3927.73	3790.69	1668.23	1685.98

dimer accurately using only ab initio data. We have used the CCSD(T)/aug-cc-pVQZ ab initio method, which is sufficiently high level for the purpose of this work. More sophisticated computations of the electronic energies would not improve the vibrational energy level results because of the approximations in the vibrational model. Our vibrational model employs a curvilinear coordinate approach that gives a simple and intuitive picture for the large amplitude motions. We have used the geometric algebra method to derive the kinetic energy operator and calculated the energies variationally using a free rotor basis for the large amplitude motion. Our calculated values show good agreement with the observed acceptor tunneling splittings for $(H_2O)_2$ and $(D_2O)_2$. Moreover, our results are close to the previously calculated acceptor tunneling splittings for $(H_2O)_2$ and $(D_2O)_2$ by Huang et al.[17]

The tunneling splittings associated with the monomer vibrational modes were simulated using a model where the low-frequency acceptor tunneling motion was adiabatically separated from the high-frequency vibrations. It was found that the change in the splittings as a function of vibrational energy are small in magnitude. The largest change occurs for the hydrogen-bonded O−H stretching vibrational mode, where the splitting decreases with increasing vibrational excitation. It is very pleasing that the simple and physically appealing adiabatic model works well in separating high-frequency O−H stretching vibrations and low-frequency tunneling motion. It is would be difficult to obtain fully converged energy level values from more sophisticated models such as full variational calculations with exact kinetic energy operators due to high density of states at high O−H stretching energies.

Acknowledgment. We thank the Academy of Finland for financial support. We also thank the CSC Scientific Computing Ltd. for providing computing time. T.S. wants to thank the University of Helsinki for a research fellowship.

Supporting Information Available: Derivation of the gradient operator used in the reciprocal tensor. This material is available free of charge via the Internet at http://pubs.acs.org.

References and Notes

(1) Stone, A. J. *The Theory of Intermolecular Forces*; Oxford University Press: Oxford, 1996.

(2) Cormier, J. G.; Hodges, J. T.; Drummond, J. R. *J. Chem. Phys.* **2005**, *122*, 114309.

(3) Sierk, B.; Solomon, S.; Daniel, J. S.; Portmann, R. W.; Gutman, S. I.; Langford, A. O.; Eubank, C. S.; Dutton, E. G.; Holub, K. H. *J. Geophys. Res.* **2004**, *109*, D08307.

(4) Burnham, C. J.; Xantheas, S. S.; Miller, M. A.; Applegate, B. E.; Miller, R. E. *J. Chem. Phys.* **2002**, *117*, 1109.

(5) Fröchtenicht, R.; Kaloudis, M.; Koch, M.; Huisken, F. *J. Chem. Phys.* **1996**, *105*, 6128.

(6) Fredin, L.; Nelander, B.; Ribbegard, G. *J. Chem. Phys.* **1977**, *66*, 4065.

(7) Perchard, J. P. *Chem. Phys.* **2001**, *266*, 109.

(8) Perchard, J. P. *Chem. Phys.* **2001**, *273*, 217.

(9) Boutellier, Y.; Perchard, J. P. *Chem. Phys.* **2004**, *305*, 1.

(10) Slipchenko, M. N.; Kuyanov, K. E.; Sartakov, B. G.; Vilesov, A. F. *J. Chem. Phys.* **2006**, *124*, 241101.

(11) Buck, U.; Huisken, F. *Chem. Rev.* **2000**, *100*, 3863.

(12) Paul, J. B.; Collier, C. P.; Saykally, R. J.; Scherer, J. J.; O'Keefe, A. *J. Phys. Chem. A* **1997**, *101*, 5211.

(13) Paul, J. B.; Provencal, R. A.; Petterson, A.; Saykally, R. J. *J. Chem. Phys.* **1998**, *109*, 10201.

(14) Paul, J. B.; Provancal, R. A.; Chapo, C.; Roth, K.; Casaes, R.; Saykally, R. J. *J. Phys. Chem. A* **1999**, *103*, 2927.

(15) Huang, Z. S.; Miller, R. E. *J. Chem. Phys.* **1989**, *91*, 6613.

(16) Nizkorodov, S. A.; Ziemkiewicz, M.; Nesbitt, D. J. *J. Chem. Phys.* **2005**, *122*, 194316–1.

(17) Huang, X.; Braams, B. J.; Bowman, J. M.; Kelly, R. E. A.; Tennyson, J.; Groenenbloom, G. C.; van der Avoird, A. *J. Chem. Phys.* **2008**, *128*, 034312–1.

(18) Huisken, F.; Kaloudis, M.; Kulcke, A. *J. Chem. Phys.* **1996**, *104*, 17.

(19) Ptashnik, I. V.; Smith, K. M.; Shine, K. P.; Newnham, D. A. *Q. J. R. Meteorol. Soc.* **2004**, *130*, 2391.

(20) Daniel, J. S.; Solomon, S.; Sanders, R. W.; Portman, R. W.; Miller, D. C.; Madsen, W. *J. Geophys. Res.* **1999**, *104*, 16785.

(21) Hill, C.; Jones, R. L. *J. Geophys. Res.* **2000**, *105*, 9421.

(22) Pfeilsticker, K.; Lotter, A.; Peters, C.; Bösch, H. *Science* **2003**, *300*, 2078.

(23) Suhm, M. A. *Science* **2004**, *304*, 823.

(24) Pfeilsticker, K. *Science* **2004**, *304*, 824.

(25) Paynter, D.; Ptashnik, I.; Shine, K.; Smith, K. *Geophys. Res. Lett.* **2007**, *34*, L12808.

(26) Leforestier, C.; Gatti, F.; Fellers, R. S.; Saykally, R. J. *J. Chem. Phys.* **2002**, *117*, 8710.

(27) Hänninen, V.; Horn, M.; Halonen, L. *J. Chem. Phys.* **1999**, *111*, 3018.

(28) Hänninen, V.; Halonen, L. *J. Chem. Phys.* **2007**, *126*, 064309.

(29) Howard, D. L.; Robinson, T. W.; Fraser, A. E.; Kjaergaard, H. G *Phys. Chem. Chem. Phys.* **2004**, *6*, 719.

(30) Halonen, L. *Adv. Chem. Phys.* **1998**, *104*, 41.

(31) Wang, X.; Perry, D. S. *J. Chem. Phys.* **1998**, *109*, 10795.

(32) Pesonen, J.; Miani, A.; Halonen, L. *J. Chem. Phys.* **2001**, *115*, 1243.

(33) Wilson, E. B.; Decius, J. C.; Cross, P. C. *Molecular Vibrations*; Dover: New York, 1980.

(34) Pesonen, J. *J. Chem. Phys.* **2000**, *112*, 3121.

(35) Pesonen, J.; Halonen, L. *Adv. Chem. Phys.* **2003**, *125*, 269.

(36) Smith, B. J.; Swanton, D. J.; Pople, J. A.; Schaefer, H. F.; Radom, L. *J. Chem. Phys.* **1990**, *92*, 1240.

(37) Goldman, N.; Fellers, R. S.; Brown, M. G.; Braly, L. B.; Keoshian, C. J.; Leforestier, C.; Saykally, R. J. *J. Chem. Phys.* **2002**, *116*, 10148.

(38) Kjaergaard, H. G.; Garden, A. L.; Chaban, G. M.; Gerber, R. B.; Matthews, D. A.; Stanton, J. F. *J. Phys. Chem. A* **2008**, *112*, 4324.

(39) Low, G. R.; Kjaergaard, H. G. *J. Chem. Phys.* **1999**, *110*, 9104.

(40) Salmi, T.; Hänninen, V.; Garden, A. L.; Kjaergaard, H. G.; Tennyson, J.; Halonen, L. *J. Phys. Chem. A* **2008**, *112*, 6305.

(41) Kendall, R. A.; Dunning, T. H., Jr.; Harrison, R. J. *J. Chem. Phys.* **1992**, *96*, 6769.

(42) Dunning, T. H., Jr. *Chem. Phys.* **1989**, *90*, 1007.

(43) Schofield, D. P.; Kjaergaard, H. G. *Phys. Chem. Chem. Phys.* **2003**, *5*, 3100.

(44) Werner, H.-J.; Knowles, P. J.; Lindh, R.; Manby, F. R.; Schütz, M.; et al. MOLPRO, version 2006.1, a package of ab initio programs, 2006, see http://www.molpro.net.

(45) Morse, P. M. *Phys. Rev.* **1929**, *34*, 57.

JP901974Z